Inorg. Chem. **2007**, *46*, 5882–5892

EXAFS Investigation of U(VI), U(IV), and Th(IV) Sulfato Complexes in Aqueous Solution

Christoph Hennig,* Katja Schmeide, Vinzenz Brendler, Henry Moll, Satoru Tsushima, and Andreas C. Scheinost

Forschungszentrum Dresden-Rossendorf, Institute of Radiochemistry, P.O. Box 510119, 01314 Dresden, Germany

Received October 15, 2006

The local structure of U(VI), U(IV), and Th(IV) sulfato complexes in aqueous solution was investigated by U-L_3 and Th-L_3 EXAFS spectroscopy for total sulfate concentrations $0.05 \leq [SO_4^{2-}] \leq 3$ M and $1.0 \leq$ pH ≤ 2.6. The sulfate coordination was derived from U–S and Th–S distances and coordination numbers. The spectroscopic results were combined with thermodynamic speciation and density functional theory (DFT) calculations. In equimolar $[SO_4^{2-}]/[UO_2^{2+}]$ solution, a U–S distance of 3.57 ± 0.02 Å suggests monodentate coordination, in line with UO_2SO_4(aq) as the dominant species. With increasing $[SO_4^{2-}]/[UO_2^{2+}]$ ratio, an additional U–S distance of 3.11 ± 0.02 Å appears, suggesting bidentate coordination in line with the predominance of the $UO_2(SO_4)_2^{2-}$ species. The sulfate coordination of Th(IV) and U(IV) was investigated at $[SO_4^{2-}]/[M(IV)]$ ratios ≥ 8. The Th(IV) sulfato complex comprises both, monodentate and bidentate coordination, with Th–S distances of 3.81 ± 0.02 and 3.14 ± 0.02 Å, respectively. A similar coordination is obtained for U(IV) sulfato complexes at pH 1 with monodentate and bidentate U–S distances of 3.67 ± 0.02 and 3.08 ± 0.02 Å, respectively. By increasing the pH value to 2, a U(IV) sulfate precipitates. This precipitate shows only a U–S distance of 3.67 ± 0.02 Å in line with a monodentate linkage between U(IV) and sulfate. Previous controversially discussed observations of either monodentate or bidentate sulfate coordination in aqueous solutions can now be explained by differences of the $[SO_4^{2-}]/[M]$ ratio. At low $[SO_4^{2-}]/[M]$ ratios, the monodentate coordination prevails, and bidentate coordination becomes important only at higher ratios.

Introduction

Sulfate is able to form strong complexes with uranium and thorium, thereby affecting speciation and migration of these radionuclides in the subsurface environment. Technical processing of uranium ores with sulfuric acid drastically increases the sulfate concentrations in affected groundwaters, producing high amounts of uranium sulfate near tailings. Another artificial source of uranium sulfate is in situ leaching of uranium ore, so-called solution mining, where a leaching liquid like sulfuric acid or ammonium carbonate is injected into the ore deposit and the uranium bearing liquid is pumped back. Such in situ leaching is, or has been, applied in the U.S. (Wyoming, Nebraska, and Texas), Australia (Beverley and Honeymoon), China (Tengchong and Yining), Russia (Dalmatovkoye), Ukraine (Devladove, Bratske, and Safonovskoye), Bulgaria (Orlov Dol and Selishte), Czech Republic (Stráz pod Ralskem), and other places in the world. The risk of in situ leaching technology is that the leaching liquid migrates out of the mining zone and contaminates drinking water reservoirs. For example, in situ leaching of uranium from sandstone with sulfuric acid, applied in the Königstein uranium mine (Saxony, Germany) between 1984 and 1990,[1] resulted in contamination risk of an aquifer used for the drinking water supply of the Dresden area. Such problems are the motivation to gain better insight in the general complexation behavior of U(VI), U(IV), and Th(IV) sulfato complexes in aqueous solution. The knowledge of interactions between sulfate and these radionuclides is necessary to predict their migration capability into aquifers. This includes a description of the chemical behavior of

* To whom correspondence should be addressed. E-mail: hennig@esrf.fr.

(1) Zeissler, K. O.; Nindel, K.; Hertwig, T. In *Uranium Mining and Hydrogeology IV*; Merkel, B. J., Hasche-Berger, A., Eds.; Technische Universität Bergakademie Freiberg: Freiberg, Germany, 2005; p 713.

10.1021/ic0619759 CCC: $37.00
Published on Web 06/20/2007

Scheme 1

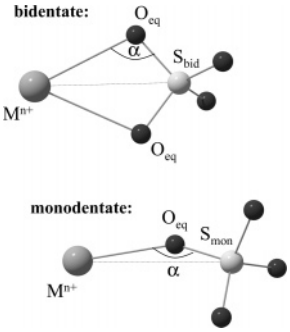

uranium sulfate under oxic and anoxic conditions which can be modeled by variation of the redox potential.

The migration of uranium in the environment is influenced by pH, the redox potential of the solutions, and the availability of potential complexation agents. In its oxidized state, U(VI) is highly soluble under acidic and alkaline conditions. Under anoxic conditions, U(IV) precipitates easily except for strongly acidic conditions. At neutral pH and under reduced conditions, uranium is almost immobile. In situ leaching with sulfuric acid creates a low pH in the concerned area keeping uranium sulfate soluble even under reduced conditions.

Sulfate is a moderately strong base and is thus partly protonated at low pH. The uranyl ion, UO_2^{2+}, forms binary sulfato complexes in slightly acidic solution. Thermodynamic data are available for three sulfato species, UO_2SO_4(aq), $UO_2(SO_4)_2^{2-}$, and $UO_2(SO_4)_3^{4-}$.[2,3] At pH values >3, hydrolysis of uranyl causes formation of various oligomeric species comprising bridging hydroxide/oxide and sulfate ligands. The major ternary complexes found so far are $(UO_2)_2(OH)_2(SO_4)_2^{2-}$, $(UO_2)_3(OH)_4(SO_4)_3^{4-}$, and $(UO_2)_5(OH)_8(SO_4)_n^{2-2n}$, with $n = 5$ or 6.[4,5] However, the most recent NEA database for uranium[3] does not consider them to be proven yet.

For U(IV), the actual NEA thermodynamic database reports only two sulfate species reported for U(IV), USO_4^{2+}, and $U(SO_4)_2$(aq).[3] For Th(IV) there are no commonly agreed thermodynamic data available for Th(IV) (a NEA review volume is in preparation). Important sulfate species in the acidic pH range include $ThSO_4^{2+}$, $Th(SO_4)_2$(aq), $Th(SO_4)_3^{2-}$, and $Th(SO_4)_4^{4-}$.[6]

Sulfate is able to coordinate either in monodentate or bidentate arrangements (Scheme 1). X-ray diffraction studies of U(VI) sulfates indicate, that monodentate sulfate ligands typically show U−S_{mon} distances in the range of 3.57−3.68 Å and short U−O_{eq} distance of 2.30−2.37 Å. Sulfate in bidentate arrangement shows U−S_{bid} distances in the range of 3.09−3.10 Å and longer U−O_{eq} distances of 2.42−2.48 Å. The angle α is 138−147° for monodentate and 96−105° for bidentate sulfate arrangement. Typical bond lengths of U(VI), U(IV), and Th(IV) are given in the Supporting Information (Tables S3 and S4).

Thermodynamic speciation provides the complex stoichiometry but does not reveal the coordination mode of the sulfate ligands. The structure of uranium and thorium sulfato species in aqueous solution is still under debate. Evidence for bidentate U(VI) sulfate coordination at high sulfate concentrations was found up to pH 5 by EXAFS.[7] A similar result, indicating a bidentate coordination mode of sulfate, was obtained with Raman spectroscopy for a high $[SO_4^{2-}]/[UO_2^{2+}]$ ratio at pH 2.[8] In this study, the existence of UO_2SO_4(aq) (860 cm^{-1}), $UO_2(SO_4)_2^{2-}$ (852 cm^{-1}), and $UO_2(SO_4)_3$ (843 cm^{-1}) was assumed from the frequency shift. In contrast, monodentate sulfate coordination to uranyl units has been suggested by infrared spectroscopy.[9] This observation was confirmed by high-energy X-ray scattering (HEXS) for equimolar $[SO_4^{2-}]/[UO_2^{2+}]$ solutions.[10] Recent quantum chemical calculations on uranyl sulfate assume bidentate sulfate coordination.[11] The comparison of these references gives a contradicting impression on the sulfate coordination mode of UO_2^{2+}. Structural investigations of Th(IV) and U(IV) aquo sulfato species are missing in the literature up to now.

Extended X-ray absorption fine structure (EXAFS) spectroscopy is an established technique for the determination of the coordination in aqueous solution.[12] Due to its element selectivity, the analysis of coordination allows the determination of solution species in complex matrices. Our study intends to clarify the discrepancies of reported results on the structure of the U(VI) sulfato complexes and to elucidate the structural features for Th(IV) and U(IV) sulfato species. For the U(VI) sulfato complexes, DFT calculations were applied to compare the total bonding energy of different structural isomers. The species with the stable oxidation states, U(VI) and Th(IV), will be discussed first, followed by U(IV).

Experimental Section

Sample Preparation. A summary of the samples investigated by EXAFS spectroscopy is given in Table 1. Details of the preparation are given below.

U(VI) and U(IV) Hydrate. UO_3 was obtained by heating $UO_2(NO_3)_2 \cdot nH_2O$ (Lachema) at 300 °C for 2 days. A U(VI) stock solution (0.1 M) was prepared by dissolving UO_3 in 0.3 M $HClO_4$. The solution of U(VI) hydrate (sample **A**) was prepared by adding

(2) Geipel, G.; Brachmann, A.; Brendler, V.; Bernhard, G.; Nitsche, H. *Radiochim. Acta* **1996**, *75*, 199−204.
(3) Guillaumont, R.; Fanghänel, T.; Fuger, J.; Grenthe, I.; Neck, V.; Palmer, D. A.; Rand, M. H. *Update on the chemical thermodynamics of uranium, neptunium, plutonium, americium and technetium*; Elsevier Science Publishers: Amsterdam, 2003.
(4) Peterson, A. *Acta Chem. Scand.* **1961**, *15*, 101.
(5) Grenthe, I.; Lagerman, B. *Radiochim. Acta* **1993**, *61*, 169−176.
(6) Langmuir, D.; Herman, J. S. *Geochim. Cosmochim. Acta* **1980**, *44*, 1733−1766.
(7) Moll, H.; Reich, T.; Hennig, C.; Rossberg, A.; Szabo, Z.; Grenthe, I. *Radiochim. Acta* **2000**, *88*, 559−566.
(8) Nguyen-Trung, C.; Begun, G. M.; Palmer, D. A. *Inorg. Chem.* **1992**, *31*, 5280−5287.
(9) Gál, M.; Goggin, P. L.; Mink, J. *Spectrochim. Acta A* **1992**, *48*, 121−132.
(10) Neuefeind, J.; Skanthakumar, S.; Soderholm, L. *Inorg. Chem.* **2004**, *43*, 2422−2426.
(11) Craw, J. S.; Vincent, M. A.; Hillier, I. H.; Wallwork, A. L. *J. Phys. Chem. A* **1995**, *99*, 10181−10185.
(12) Antonio, M. R.; Soderholm, L. In *The Chemistry of the Actinides and Transactinides*; Springer: Dordrecht, The Netherlands, 2006; Vol. 5, pp 3086−3189.

Table 1. List of Samples[a]

ID	chemical composition	speciation	pH	$[SO_4^{2-}]$
A	0.01 M U(VI), 0.1 M $HClO_4$[b]	100% UO_2^{2+}	0.89	
B	0.05 M UO_2SO_4, 0.15 M H_2SO_4, 0.2 M $(NH_4)_2SO_4$[c]	15.7% UO_2^{2+} 26.7% UO_2SO_4(aq) 53.8% $UO_2(SO_4)_2^{2-}$ 3.1% $UO_2(SO_4)_3^{4-}$	0.96	0.4
C	0.05 M UO_2SO_4, 0.3 M H_2SO_4, 0.95 M $(NH_4)_2SO_4$[c]	3.1% UO_2^{2+} 19.4% UO_2SO_4(aq) 75.1% $UO_2(SO_4)_2^{2-}$ 2.2% $UO_2(SO_4)_3^{4-}$	1.00	1.3
D	0.05 M UO_2SO_4, 0.38 M H_2SO_4, 1.57 M $(NH_4)_2SO_4$,[c]	1.7% UO_2^{2+} 21.2% UO_2SO_4(aq) 76.2% $UO_2(SO_4)_2^{2-}$	0.99	2.0
E	0.05 M UO_2SO_4, 0.6 M H_2SO_4, 2.35 M $(NH_4)_2SO_4$[c]	25.6% UO_2SO_4(aq) 73.1% $UO_2(SO_4)_2^{2-}$	0.99	3.0
F	0.5 M U(VI), 0.5 M H_2SO_4	37.5% UO_2^{2+} 31.0% UO_2SO_4(aq) 30.0% $UO_2(SO_4)_2^{2-}$	1.96	0.5
G	0.05 M U(VI), 0.05 M H_2SO_4	42.9% UO_2^{2+} 40.3% UO_2SO_4(aq) 15.8% $UO_2(SO_4)_2^{2-}$	2.55	0.05
H	zippeite, $K(UO_2)_2SO_4(OH)_3H_2O$			
I	0.05 M Th(IV), 0.5 M $HClO_4$	100% Th^{4+}	1.00	
J	0.05 M Th(IV), 0.17 M H_2SO_4, 0.23 M $(NH_4)_2SO_4$	2.4% $ThSO_4^{2+}$ 70.8% $Th(SO_4)_2$(aq) 26.7% $Th(SO_4)_3^{2-}$	1.00	0.4
K	0.05 M Th(IV), 0.39 M H_2SO_4, 1.61 M $(NH_4)_2SO_4$	55.1% $Th(SO_4)_2$(aq) 44.7% $Th(SO_4)_3^{2-}$	1.02	2.0
L	0.01 M U(IV), prepared from **A**[b]	100% U^{4+}		
M	0.05 M U(IV), prepared from **B**[c]	3.7% USO_4^{2+} 96.3% $U(SO_4)_2$(aq)		0.4
N	0.05 M U(IV), prepared from **C**[c]	0.7% USO_4^{2+} 99.1% $U(SO_4)_2$(aq)		1.3
O	0.05 M U(IV), prepared from **D**[c]	0.5% USO_4^{2+} 99.5% $U(SO_4)_2$(aq)		2.0
P	precipitate of U(IV) sulfate			

[a] Electrolytically prepared U(IV) samples and their starting U(VI) solutions contain Cl^- ions in order to enforce the anode reaction: [b] 0.02 M LiCl, [c] 0.1 M NaCl.

aliquots of the U(VI) and $HClO_4$ stock solutions. U(IV) hydrate (sample **L**) was obtained by electrolysis of the U(VI) solution.

U(VI) and U(IV) Sulfate. A stock solution of 0.2 M uranyl sulfate was prepared by dissolving UO_3 in 0.2 M H_2SO_4. Samples **B**, **C**, **D**, and **E** were prepared by adding aliquots of stock solutions of uranyl sulfate, H_2SO_4, and solid $(NH_4)_2SO_4$. The amounts of H_2SO_4 and $(NH_4)_2SO_4$ were varied according to the values given at Table 1 to adjust the total sulfate concentration and the pH value. Samples **F** and **G** were prepared by dissolving appropriate amounts of UO_3 in H_2SO_4 to achieve equimolar concentrations of U(VI) and sulfate of 0.5 and 0.05 M, respectively. U(IV) sulfate solutions (samples **M**, **N**, **O**) were prepared by electrolysis of the corresponding U(VI) solutions.

Th(IV) Hydrate. A 0.1 M Th(IV) stock solution was obtained by dissolving $Th(NO_3)_4 \cdot 5H_2O$ in 0.5 M HCl. The Th(IV) stock solution (10 mL) was evaporated to dryness under stirring. The residue was redissolved in 10 mL of 0.5 M HCl and again evaporated to dryness. This was repeated twice. The residue was redissolved in water, and Th was precipitated with NaOH. The Th precipitate was isolated by centrifugation and washed with water several times. Subsequently, 5 mL of 1 M $HClO_4$ was added. The volume was increased to 10 mL by adding water (sample **I**). The pH value was adjusted with NaOH.

Th(IV) Sulfate. Samples **J** and **K** were prepared according to the U(VI) sulfate solutions by adding aliquots of stock solutions of $Th(NO_3)_4$, H_2SO_4, and solid $(NH_4)_2SO_4$.

U(IV) Sulfate Precipitate. The electrochemical reduction of uranyl sulfate solutions at pH ±1.5 is accompanied by a precipitation. This precipitation prevented a complete reduction of U(VI) by passivating the electrodes. In order to obtain a solid U(IV) compound, a uranyl sulfate solution was initially reduced at pH 1 (starting solution was sample **B**). Subsequently, the pH of the U(IV) sulfate solution was increased to pH 2 by adding NaOH. The precipitate (sample **P**) was separated from the solution by centrifugation and dried under inert gas atmosphere. The elemental analysis of this precipitate, determined by ICP−MS after wet digestion, is [mg/g] U, 458.0; Na, 59.7; SO_4^{2-}, 64.0. The precipitate can be regarded as amorphous because no peaks were observed with X-ray diffraction.

Zippeite. This reference sample (sample **H**), $K(UO_2)_2SO_4(OH)_3 \cdot H_2O$, was provided by R. Vochten (University of Antwerp). Its preparation and crystal structure are already described.[13]

Electrochemical Reduction. To convert uranium to its tetravalent oxidation state, we used an electrochemical cell as described previously.[14] A Pt gauze was used as working electrode. The reference potential is the Ag^+/AgCl couple. The reduction of U(VI) to U(IV) involves an electron transfer and a chemical reaction transforming the trans-dioxo cation to the spherical coordinated U^{4+} cation. The reaction at the working electrode is

$$UO_2^{2+} + 2e^- + 4H^+ \rightleftharpoons U^{4+} + 2H_2O \quad (1)$$

For security reasons, the release of any gas had to be prevented at the beam line; hence, an electrode of second kind was used as counter electrode, consisting of metallic Ag (rod of 1 mm diameter) and 0.1 M $[Cl^-]$ ions in the solution. During the uranium reduction at the cathode, twice the molar amount of Ag oxidizes to Ag^+ and reacts with Cl^- from the solution to AgCl

$$2Ag + 2Cl^- \rightleftharpoons 2AgCl\downarrow + 2e^- \quad (2)$$

The formation of the AgCl precipitate at the counter electrode prevented the reoxidation of U(IV). Since the stability constants of uranium chloro complexes are low, it can be excluded that the sulfate speciation was affected by the presence of 0.1 M $[Cl^-]$.[14]

UV−vis spectra were obtained before and after the reduction in order to verify the initial and final oxidation states. The measurements were performed in a quartz glass cuvette with an optical path length of 10 mm using a CARY-5G/Varian spectrometer. As an example, the UV−vis spectra of samples **D** and **O** are shown in Figure F1 of the Supporting Information. The spectrum of U(VI) shows the typical fine structure which is dominated by the vibration modes of the trans-dioxo cation, UO_2^{2+}. The transitions in the spectrum are mainly arising from electronic configurations of the type $(\sigma_u^+)^2 \rightarrow \sigma_u^+\delta_u$ and $(\sigma_u^+)^2 \rightarrow \sigma_u^+\phi_u$.[15] The UV−vis absorption spectrum of U(IV) sulfate shows four typical broad absorption bands with a higher oscillator strength than that of U(VI).

Sample Conditions for EXAFS Measurements. The storage of the samples with the stable oxidation states U(VI) and Th(IV)

(13) Vochten, R.; Vanhaverbeke, L.; Vanspringel, K.; Blaton, N.; Peeters, O. M. *Canad. Min.* **1995**, *33*, 1091−1101.
(14) Hennig, C.; Tutschku, J.; Rossberg, A.; Bernhard, G.; Scheinost, A. C. *Inorg. Chem.* **2005**, *44*, 6655−6661.
(15) Servaes, K.; Hennig, C.; Van, Deun, R.; Görller-Walrand, C. *Inorg. Chem.* **2005**, *44*, 7705−7707.

did not need any specific precautions. However, different U and Th concentrations required individually adapted optical path lengths for the sample vials to obtain similar noise levels of the EXAFS spectra. Hence, polyethylene vials with an optical path length of 3 and 13 mm were used for the samples with 0.5 and 0.05 M U and Th, respectively, encapsulated in 200 μm polyethylene film as second confinement against radionuclide release. In situ EXAFS measurements with the spectroelectrochemical cell with an optical path length of 20 mm were applied to obtain spectra of U(IV) hydrate as described previously.[14] The U(VI) → U(IV) reduction was performed under inert gas atmosphere in the electrochemical cell. The EXAFS measurement of the U(IV) hydrate (sample **L**) was performed in situ, whereas the U(IV) sulfate solutions were transferred from the electrochemical cell into quartz glass cuvettes (optical path length of 10 mm). The solid samples were measured as powder pellet (**H**) and wet paste (**P**) in hot-sealed polyetylene cuvettes.

EXAFS Data Acquisition. EXAFS measurements were carried out at the Rossendorf Beamline[16] at the European Synchrotron Radiation Facility. The monochromator, equipped with a Si(111) double crystal, was used in channel-cut mode. Higher harmonics were rejected by two Pt-coated mirrors. All experiments were performed at room temperature. The spectra were collected in transmission mode using argon-filled ionization chambers. Across the EXAFS region, data points were collected with equidistant k steps of 0.05 Å^{-1}. The monochromator energy scale was calibrated to the K-edge of an Y metal foil (first inflection point assigned to 17038 eV).

EXAFS Data Analysis. The EXAFS oscillations were extracted from the raw absorption spectra by standard methods including a μ_0 spline approximation for the atomic background using either the WINXAS[17] or the EXAFSPAK[18] software packages. A square window function has been applied for the Fourier transform. In order to suppress side lobe effects, care has been taken to keep $\chi(k) \approx 0$ at k_{min} and k_{max}. The EXAFS data were fit using theoretical phase and amplitude functions calculated with the FEFF 8.2 code of Rehr et al.[19] The scattering interactions were calculated using single scattering (SS) and multiple scattering (MS) paths of the model compounds $Na_{10}[(UO_2)(SO_4)_4](SO_4)_2 \cdot 3H_2O$,[20] $Cs_2Th(SO_4)_3 \cdot 3H_2O$,[21] and $U(SO_4)_2 \cdot 4H_2O$[22] and the hypothetical clusters $UO_2(H_2O)_5^{2+}$,[23] $U(H_2O)_9^{4+}$,[24] and $Th(H_2O)_9^{4+}$.[24] It has been shown that the multiple scattering path U−O_{ax} in the uranyl unit is dominated by the two-fold degenerated four-legged multiple-scattering path U−O_{ax1}−U−O_{ax2}.[25] This scattering path was included in the curve fit by constraining its Debye−Waller factor and its effective pathlength to twice the values of the corresponding, freely fitted U−O_{ax} single-scattering path. Taking into account the individual noise levels at higher k values, data analysis was restricted to the k range 3.2−16.7 Å^{-1} for U(VI) and to 4.1−14.2 Å^{-1} for U(IV) and Th(IV). The distance resolution, $\Delta R = \pi/2\Delta k$, is 0.12 Å for the U(VI) spectra and 0.16 Å for U(VI) and Th(IV). The amplitude reduction factor, S_0^2, was defined as 1.0 in the FEFF calculation and fixed to that value in the data fits. The threshold energy, $E_{k=0}$, was arbitrarily defined for U(VI) and U(IV) as 17 185 eV, and for Th(IV) as 16 320 eV and varied as a global fit parameter resulting in the energy shift $\Delta E_{k=0}$. The same energy shift was applied for each shell. The overall goodness of the fits, F, is given by χ^2 weighted by the magnitude of data.[18]

Double-Electron Excitations. The excited photoelectron has a certain probability to excite a second electron into unoccupied orbitals (shake up) or the continuum (shake off). Since the intensity of double-electron excitation is usually only a few percent of a single-electron excitation, their appearance is often masked by the single-electron EXAFS oscillation. The spectra obtained from solutions show weak EXAFS amplitudes, especially at high k values, and therefore, double-electron excitations become more dominant. The EXAFS data shown here are partly affected by [2p4f] double-electron excitations.[26] The spectra of Th(IV) and U(IV) are more affected than the spectra of U(VI) due to stronger resonance intensity of their double-electron excitations.[26] While the double-electron excitation may bias the EXAFS amplitude and hence the coordination numbers and Debye−Waller factors, the frequency of the main electron excitation channel is not affected; hence, the determined distances are not influenced. Deviations between $\mu_0(E)$ and its spline approximation lead to artificial peaks at $R \leq 1.2$ Å, which were minimized during the data extraction. The double-electron excitation itself acts as a high-frequency feature that may contribute spurious peaks at large R values. Fourier filtering procedures and data analysis using reduced k ranges indicated that the effects are small and within the usual error limits. Therefore, for the final data analysis, the raw data itself and not the Fourier-filtered data were used. In Figures 4, 6 and 7, double-electron excitations are marked with a dotted line and their k values are given. A more detailed discussion of double-electron excitation phenomena in L_3-edge X-ray absorption spectra of actinides is given elsewhere.[26]

Quantum Chemical Calculations. The quantum chemical calculations were performed at the B3LYP level in the aqueous phase without any symmetry constraints using the Gaussian 03 program package.[27] The energy-consistent small-core effective core potential (ECP) and the corresponding basis set suggested by Dolg

(16) Matz, W.; Schell, N.; Bernhard, G.; Prokert, F.; Reich, T.; Claussner, J.; Oehme, W.; Schlenk, R.; Dienel, S.; Funke, H.; Eichhorn, F.; Betzl, M.; Prohl, D.; Strauch, U.; Huttig, G.; Krug, H.; Neumann, W.; Brendler, V.; Reichel, P.; Denecke, M. A.; Nitsche, H. *J. Synchr. Rad.* **1999**, *6*, 1076−1085.

(17) Ressler, T. *J. Synchr. Rad.* **1998**, *5*, 118−122.

(18) George, G. N.; Pickering, I. J. *EXAFSPAK, a suite of computer programs for analysis of X-ray absorption spectra*; Stanford University: Stanford, CA, 2000.

(19) Rehr, J. J.; Albers, R. C. *Rev. Mod. Phys.* **2000**, *72*, 621−654.

(20) Burns, P. C.; Hayden, L. A. *Acta Crystallogr. C* **2002**, *58*, i121−i123.

(21) Habash, J.; Smith, A. J. *J. Cryst. Spec. Res.* **1992**, *22*, 21−24.

(22) Kierkegaard, P. *Acta Chem. Scand.* **1956**, *10*, 599−616.

(23) Tsushima, S.; Yang, T. X.; Suzuki, A. *Chem. Phys. Lett.* **2001**, *334*, 365−373.

(24) Tsushima, S.; Yang, T. X. *Chem. Phys. Lett.* **2005**, *401*, 68−71.

(25) Hudson, E. A.; Rehr, J. J.; Bucher, J. J. *Phys. Rev. B* **1995**, *52*, 13815−13826.

(26) Hennig, C. *Phys. Rev. B* **2007**, *75*, 035120−035126.

(27) Frisch, M. J.; Trucks, G. W.; Schlegel, H. B.; Scuseria, G. E.; Robb, M. A.; Cheeseman, J. R.; Montgomery, J. A., Jr.; Vreven, T.; Kudin, K. N.; Burant, J. C.; Millam, J. M.; Iyengar, S. S.; Tomasi, J.; Barone, V.; Mennucci, B.; Cossi, M.; Scalmani, G.; Rega, N.; Petersson, G. A.; Nakatsuji, H.; Hada, M.; Ehara, M.; Toyota, K.; Fukuda, R.; Hasegawa, J.; Ishida, M.; Nakajima, T.; Honda, Y.; Kitao, O.; Nakai, H.; Klene, M.; Li, X.; Knox, J. E.; Hratchian, H. P.; Cross, J. B.; Bakken, V.; Adamo, C.; Jaramillo, J.; Gomperts, R.; Stratmann, R. E.; Yazyev, O.; Austin, A. J.; Cammi, R.; Pomelli, C.; Ochterski, J. W.; Ayala, P. Y.; Morokuma, K.; Voth, G. A.; Salvador, P.; Dannenberg, J. J.; Zakrzewski, V. G.; Dapprich, S.; Daniels, A. D.; Strain, M. C.; Farkas, O.; Malick, D. K.; Rabuck, A. D.; Raghavachari, K.; Foresman, J. B.; Ortiz, J. V.; Cui, Q.; Baboul, A. G.; Clifford, S.; Cioslowski, J.; Stefanov, B. B.; Liu, G.; Liashenko, A.; Piskorz, P.; Komaromi, I.; Martin, R. L.; Fox, D. J.; Keith, T.; Al-Laham, M. A.; Peng, C. Y.; Nanayakkara, A.; Challacombe, M.; Gill, P. M. W.; Johnson, B.; Chen, W.; Wong, M. W.; Gonzalez, C.; Pople, J. A. *Gaussian 03*, revision C.02; Gaussian, Inc.: Wallingford, CT, 2004.

et al.[28] were used for uranium, sulfur, and oxygen, comprising 60, 10, and 2 electrons in the core, respectively. Uranium and sulfur/oxygen basis sets were supplemented with two g-functions and one d-function, respectively. For hydrogen, a 5s contracted to 3s basis set was used. All geometry optimization calculations were followed by vibrational frequency calculations to ensure that no imaginary vibrational frequency is present in optimized geometries. Presumably due to a very flat potential energy surface for a geometry optimization in solvent, we were not able to remove single and very small imaginary vibrational frequency (less than $10i$ cm^{-1}) in some of the calculations. Such small imaginary vibrational frequency is often a computational artifact, therefore considered to be unimportant. However, such imaginary vibrational frequencies are reported in the text when encountered. DFT calculations were performed only on U(VI) sulfate. For Th(IV) and U(IV), whose coordination is not restricted to an equatorial plane like in U(VI), it is difficult to find a global minimum.

Thermodynamic Data and Speciation Modeling. As pointed out in the Introduction, only a few reviewed thermodynamic data are available for the systems of interest in this work. The thermodynamic calculations of the species are based on the following complex formation constants: Guillaumont et al., 2003,[3] for U(VI) and U(IV), and Langmuir and Herman, 1980,[6] for Th(IV):

(a) Uranium(VI) log	log K^0
$UO_2^{2+} + SO_4^{2-} \rightleftarrows UO_2SO_4$(aq)	3.15
$UO_2^{2+} + 2\ SO_4^{2-} \rightleftarrows UO_2(SO_4)_2^{2-}$	4.14
$UO_2^{2+} + 3\ SO_4^{2-} \rightleftarrows UO_2(SO_4)_3^{4-}$	3.02
(b) Uranium(IV)	
$U^{4+} + SO_4^{2-} \rightleftarrows USO_4^{2+}$	6.58
$U^{4+} + 2\ SO_4^{2-} \rightleftarrows U(SO_4)_2$(aq)	10.51
(c) Thorium(IV)	
$Th^{4+} + SO_4^{2-} \times c1\ ThSO_4^{2+}$	5.31
$Th^{4+} + 2\ SO_4^{2-} \rightleftarrows Th(SO_4)_2$(aq)	9.62
$Th^{4+} + 3\ SO_4^{2-} \rightleftarrows Th(SO_4)_3^{2-}$	10.40
$Th^{4+} + 4\ SO_4^{2-} \rightleftarrows Th(SO_4)_4^{4-}$	8.40

By comparing the stability of the respective U(VI) and U(IV) complexes, it is obvious that the reduced form of uranium has a stronger affinity toward the sulfate anion than the oxidized form. Thus, the presence of sulfate promotes the stability of the reduced uranium species. The stability is especially significant for the disulfato complex. Hence, the EXAFS measurements of U(IV) sulfate solutions did not required the use of an in situ electrochemical technique. The strength of the Th−sulfate interaction is slightly weaker than that of U(IV), but still much stronger than that of U(VI).

The thermodynamic calculation considered all ions in the solution including NH_4^- and Cl^-. With increasing ammonium sulfate concentration, the $NH_4SO_4^-$ ion pair becomes more important.[29] It is hence advisable to relate the extent to which the various uranyl sulfate complexes are formed to the free sulfate concentration rather than to the total concentration because certain amounts of sulfate are bound by HSO_4^- or $NH_4SO_4^-$. Nevertheless, there is enough free sulfate available to maintain a high $[SO_4^{2-}]/[UO_2^{2+}]$ ratio. The high ionic strength used for the sample preparation is above the validity limit of the extended Debye−Hückel formalisms commonly used to correct activity coefficients. From the variety of more appropriate models, only two have been applied widely enough to provide significant parameter sets: The specific ion interaction theory (SIT)[30,31] and the Pitzer model.[32] However, for the systems considered here, with NaCl as electrolyte for the electrode of second kind and significant amounts of ammonia, the parametrization is still insufficient. Closing this gap with estimates and chemical analogies would probably introduce errors of the same order of magnitude as when applying simpler activity coefficient models. Hence, the speciation calculations were performed with EQ3/6 applying the Davies equation for activity coefficients.[33] The speciation results are given at Table 1 and discussed in the following together with the structural aspects.

Results and Discussion

U(VI) Complexes. UO_2SO_4(aq), $UO_2(SO_4)_2^{2-}$, and $UO_2(SO_4)_3^{4-}$ cannot be prepared individually because they exist always in equilibrium with other species. UO_2SO_4(aq) is dominant at equimolar $[SO_4^{2-}]/[UO_2^{2+}]$ solution. $UO_2(SO_4)_2^{2-}$ is dominant at low pH and sulfate excess. $UO_2(SO_4)_3^{4-}$ is always only a minor component. At higher pH and sulfate concentration, where it may exist to a larger extend,[2] hydrolysis species and ternary complexes are ubiquitous.[7,34] U(VI) sulfato complexes were studied here under two conditions: in excess of sulfate and in equimolar solutions. The pH was restricted to low values to inhibit the formation of ternary species. The spectrum of U(VI) hydrate was included as reference. All figures show the raw data (line) and the shell-fit (dots). The Fourier transform (FT) of the EXAFS data represents a pseudoradial distribution function, where peaks are shifted to lower values $R + \Delta$ relative to the true near-neighbor distances, R. This Δ shift of -0.2 to -0.5 Å depends on the scattering behavior of the electron wave in the atomic potentials and was treated as a variable during the shell fits. FT peaks at $R + \Delta < 1.2$ Å are typical artifacts from the spline removal procedure and are not related to structural features.

U(VI) Hydrate. The isolated k^3-weighted EXAFS data of U(VI) hydrate (sample **A**) and their corresponding FT are shown in Figure 1, the fit results are given in Table 2. The FT is dominated by the backscattering signal from the two axial oxygen atoms (O_{ax}) at a distance of 1.76 Å and from five equatorial oxygen atoms (O_{eq}) at a distance of 2.41 Å. This result is consistent with the structure previously obtained for the hydrated uranyl ion, $UO_2(H_2O)_5^{2+}$.[35−37] The O_{eq} peak shows a significant splitting, suggesting the presence of two distinct O_{eq} distances. A careful investigation of this feature revealed that the peak at $R + \Delta = 1.7$ Å originates from a superposition of the O_{eq} shell with a side lobe of the O_{ax}

(28) Dolg, M.; Wedig, U.; Stoll, H.; Preuss, H. *J. Chem. Phys.* **1987**, *86*, 866.
(29) Smith, A. J.; Martell, A. E.; Motekaitis, R. J. *NIST Critically Selected Stability Constants of Metal Complexes, Database 46, Version 4.0*; NIST: Gaithersburg, MD, 1997.
(30) Guggenheim, E. A. *Applications of Statistical Mechanics*; Clarendon Press: Oxford, 1966.
(31) Grenthe, I.; Plyasunov, A. V.; Spahiu, K. *Estimation of medium effects on thermodynamic data*; OECD, NEA: Paris, 1997.
(32) Pitzer, K. S. *J. Chem. Phys.* **1973**, *77*, 268−277.
(33) Davies, C. W. *Ion Association*; Butterworths: Washington, 1962.
(34) Comarmond, M. J.; Brown, P. L. *Radiochim. Acta* **2000**, *88*, 573−577.
(35) Vallet, V.; Wahlgren, U.; Schimmelpfennig, B.; Szabo, Z.; Grenthe, I. *J. Am. Chem. Soc.* **2001**, *123*, 11999−12008.
(36) Semon, L.; Boehme, C.; Billard, I.; Hennig, C.; Lützenkirchen, K.; Reich, T.; Rossberg, A.; Rossini, I.; Wipff, G. *Chem. Phys. Chem.* **2001**, *2*, 591−598.
(37) Neuefeind, J.; Soderholm, L.; Skanthakumar, S. *J. Phys. Chem. A* **2004**, *108*, 2733−2739.

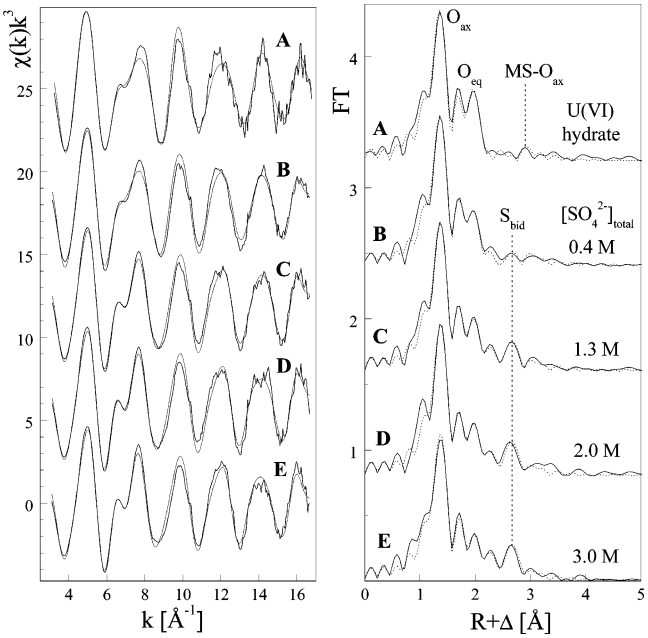

Figure 1. U L_3-edge k^3-weighted EXAFS data (left) and the corresponding Fourier transforms (right) of U(VI) hydrate and bidentate sulfato species.

Table 2. EXAFS Fit Parameters of U(VI) Hydrate and Sulfato Complexes

sample	scattering path	R [Å]	N	σ^2 [Å^2]	$\Delta E_{k=0}$	F
A	U−O_{ax}	1.76	2.0	0.0016	2.1	0.21
	U−O_{eq}	2.41	5.2	0.0071		
B	U−O_{ax}	1.77	2.0	0.0016	3.9	0.16
	U−O_{eq1}	2.35	2.5	0.0055[a]		
	U−O_{eq2}	2.47	2.1	0.0055[a]		
	U−S_{bid}	3.09	0.6	0.0060[a]		
C	U−O_{ax}	1.77	1.9	0.0014	4.0	0.15
	U−O_{eq1}	2.35	2.4	0.0055[a]		
	U−O_{eq2}	2.48	2.2	0.0055[a]		
	U−S_{bid}	3.11	1.6	0.0060[a]		
D	U−O_{ax}	1.77	1.9	0.0014	4.1	0.16
	U−O_{eq1}	2.35	2.4	0.0055[a]		
	U−O_{eq2}	2.49	2.5	0.0055[a]		
	U−S_{bid}	3.12	1.9	0.0060[a]		
E	U−O_{ax}	1.77	2.0	0.0014	4.2	0.16
	U−O_{eq1}	2.35	2.5	0.0055[a]		
	U−O_{eq2}	2.49	2.4	0.0055[a]		
	U−S_{bid}	3.12	2.0	0.0060[a]		

[a] Value fixed during the fit procedure. Errors in distances R are ±0.02 Å, errors in coordination numbers N are ±15%.

shell (for details, see Supporting Information Figure F2). In confirmation, this double peak was reliably fitted with only one shell.

U(VI) Sulfate with Excess Sulfate. Species distribution of U(VI) in solutions with an excess of sulfate is dominated by $UO_2(SO_4)_2^{2-}$. The species $UO_2(H_2O)_5^{2+}$, UO_2SO_4(aq), and $UO_2(SO_4)_3^{4-}$ are present as accessory species only (Table 1). All complexes were stable in solution; no precipitation was observed.

Figure 1 shows the EXAFS spectra of a sample series at pH 1 (samples **B**−**E**) with total sulfate concentrations from 0.4 to 3.0 M. The EXAFS spectra of an additional sample series at pH 2 (samples **Q**−**S**) is given in the Supporting Information (Figure F3 and Tables S1 and S2). The O_{eq} shell of the uranyl sulfate samples shows a splitting ($R + \Delta \approx$ 1.7 and 1.9 Å) which appears to be similar to that of uranyl hydrate at a first glance, and a new O_{eq} peak occurs at $R + \Delta \approx 2.3$ Å. In comparison with the hydrate, there is a slight intensity drop of the O_{eq} peaks at $R + \Delta \approx 1.9$ Å. A quantitative analysis, performed with fixed Debye−Waller factors $\sigma^2_{Oeq} = 0.0055$ Å,^{2} reveals two dominating U−O_{eq} distances at 2.35 and 2.47−2.49 Å. A O_{eq} coordination number of 5 or 6 is most likely, whereas a 4-fold coordination is related to a significant shorter bond length of 2.28−2.30 Å.[12,38] EXAFS reflects only the average coordination and is usually not able to differentiate between coexisting species with similar structure. Therefore, the O_{eq} distances given here are not appropriate to gain insights into the sulfate coordination.

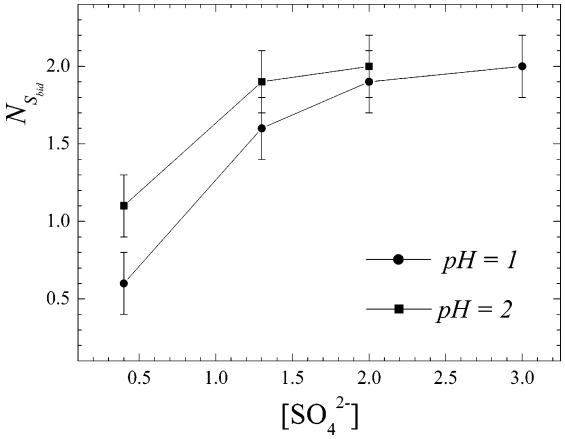

Figure 2. U(VI) sulfate coordination. Number of sulfur neighbors N_{Sbid} as function of $[SO_4^{2-}]$ at pH 1 and 2.

The coordination of sulfate can be derived from the sulfur peak because this peak is hardly affected by other scattering contributions. The U−S bond length indicates the mode of coordination, i.e., monodentate or bidentate, and its average coordination number. The FT of the samples **B**−**E** shows a well-pronounced backscattering peak from sulfur at $R + \Delta \approx 2.7$ Å. This peak was fitted with U−S distances of 3.09−3.12 Å (Table 2). The obtained distance is in agreement with bidentate sulfate coordination. For instance, bidentate-coordinated sulfate in crystal structures has U−S distances of 3.09−3.10 Å (Supporting Information, Table S3). Beside the U−O_{eq} distances of 2.35 Å, there is no indication of monodentate sulfate in the EXAFS data. A free fit of S_{bid} of sample **E** gives a Debye−Waller factor of 0.006 Å.^{2} Assuming that we have always the same sulfate coordination structure, we fixed the Debye−Waller factor in all subsequent fits. Figure 2 shows the number of sulfur neighbors, N_{Sbid}, as a function of the total sulfate concentration, with pH 1 and 2 and a $[SO_4^{2-}]/[UO_2^{2+}]$ ratio between 8 and 60. As the total sulfate concentration increases, the coordination number N_{Sbid} increases from 0.6 to 2.0. Hence, for the higher sulfate concentration, two bidentate sulfate groups are involved in the U(VI) coordination. The observed structural data from EXAFS are in line with thermodynamic data, insofar as the

(38) Hennig, C.; Reck, G.; Reich, T.; Rossberg, A.; Kraus, W.; Sieler, J. *Z. Krist.* **2003**, *218*, 37−45.

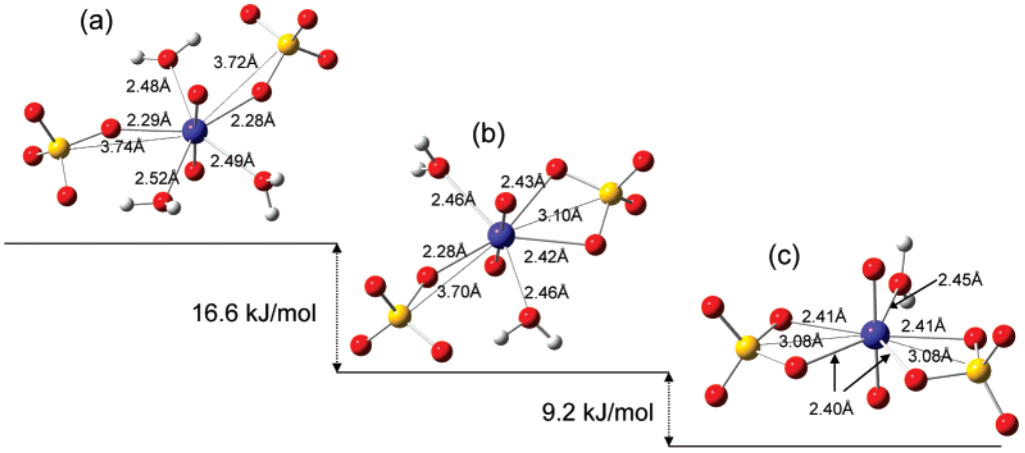

Figure 3. Structures of $UO_2(SO_4)_2(H_2O)_n^{2-}$ complexes with $N_{Oeq} = 5$ optimized at the DFT level in solvent.

coordination number N_{Sbid} reaches a maximal value of ~2 at $[SO_4^{2-}] \geq 1.3$ M, in agreement with the calculated predominance of the $UO_2(SO_4)_2^{2-}$ species and minor importance of the other species (Table 1).

Possible isomeric structures of the $UO_2(SO_4)_2^{2-}$ species at the same conditions as the experimental aqueous solution were investigated by DFT calculations. A comparison of the estimated distances from DFT and EXAFS may reveal the coordination mode. Species with a coordination number 6, e.g., $UO_2(SO_4)_2(H_2O)_2^{2-}$ and $UO_2(SO_4)_3^{4-}$ (Figure F4 of Supporting Information), are rather unlikely because the U−O_{eq} and U−S_{bid} distances obtained with DFT are too long in comparison with the values from EXAFS. Figure 3a−c shows three different $UO_2(SO_4)_2^{2-}$ complexes with a coordination number 5 in the equatorial plane comprising two bidentate sulfate groups, two monodentate groups, and one bidentate and one monodentate sulfate group, all with additional water molecules in the first coordination shell. In order to make two molecules comparable in energy, additional water molecules were added in the second coordination sphere (Figure F5 of the Supporting Information). Complex $UO_2(SO_4)_2(H_2O)_2^{2-}$ in Figure 3b has a small imaginary frequency of 2.9*i* cm^{-1}. The minimum of the Gibbs energy indicates that a coordination of two bidentate sulfate groups instead of one or two monodentate groups prevails in $UO_2(SO_4)_2^{2-}$. The U−S_{bid} distance obtained from DFT calculation for $UO_2(SO_4)_2(H_2O)^{2-}$ (Figure 3c) is 3.08 Å, which agrees fairly well with EXAFS results of 3.09−3.12 Å. The oxygen atoms, linking U and S, show a U−O_{eq} distance of 2.40−2.41 Å in the DFT. This value is significantly shorter than the average U−O_{eq} distances of 2.45−2.48 Å obtained in crystal structures (Supporting Information, Table S3). The U−O_{eq} distance for water molecules obtained from DFT calculation for the different structures is 2.45−2.49 Å, thereby suggesting that the electrostatic interaction of water in the sulfato complexes is weaker than in the pure U(VI) hydrate.

U(VI) with Equimolar Sulfate. In aqueous solution with an equimolar ratio of 0.5 M U(VI) and $[SO_4^{2-}]$, Neuefeind et al.[10] observed with HEXS exclusively monodentate sulfate coordination. We repeated this measurement with EXAFS using an identical experimental conditions of 0.5 M U(VI) (sample **F**). A second sample with a U(VI) concentration of 0.05 M (sample **G**) was prepared in order to make the result comparable with the previously discussed samples **B**−**E**. Despite the expected differences in the water activity and its influence on the coordination, both spectra and their FTs are nearly identical (Figure 4, Table 3). In contrast to Neuefeind et al.[10] we observed both monodentate and bidentate sulfate coordination. Bidentate sulfate is less pronounced ($N_{bid} \approx 0.3$) but shows a typical U−S bond length of 3.07−3.11 Å. The monodentate sulfate ($N_{mon} \approx 0.5-0.6$) has a U−S distance of 3.57 Å. In order to verify that the relatively weak signal intensity and the superposition with the U−O_{ax} multiple-scattering path did not bias the U−S_{mon} contribution, we performed an EXAFS measurement of zippeite (sample **H**). Zippeite, $K(UO_2)_2SO_4(OH)_3 \cdot H_2O$, contains exclusively monodentate sulfate with an average U−S_{mon} distance of 3.58 Å.[39,40] In good agreement with the

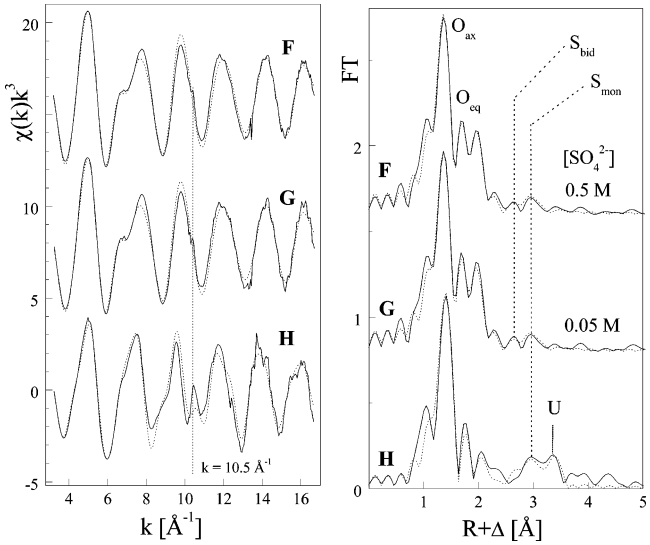

Figure 4. U L_3-edge k^3-weighted EXAFS data (left) and the corresponding Fourier transforms (right) of zippeite (**H**) and predominantly monodentate U(VI) sulfato species in equimolar $[UO_2^{2+}]/[SO_4^{2-}]$ solution. The dotted line in the EXAFS spectrum indicates the [2p4f] double-electron excitation.

(39) Vochten, R.; Vanhaverbeke, L.; Vanspringel, K.; Blaton, N.; Peeters, O. M. *Can. Mineral.* **1995**, *33*, 1091−1101.

Table 3. EXAFS Fit Parameters of U(VI) Sulfato Complexes in Equimolar $[SO_4^{2-}]/[UO_2^{2+}]$ Solutions and Zippeite

sample	scattering path	R [Å]	N	σ^2 [Å^2]	$\Delta E_{k=0}$	F
F	U−O_{ax}	1.77	1.9	0.0014	4.9	0.11
	U−O_{eq1}	2.39	4.4	0.0073		
	U−O_{eq2}	2.51	1.4	0.0073		
	U−S_{bid}	3.11	0.3	0.006*		
	U−S_{mon}	3.57	0.6	0.009*		
G	U−O_{ax}	1.77	1.9	0.0014	4.3	0.14
	U−O_{eq1}	2.39	4.2	0.0076		
	U−O_{eq2}	2.50	0.8	0.0076		
	U−S_{bid}	3.07	0.3	0.006*		
	U−S_{mon}	3.56	0.5	0.009*		
H	U−O_{ax}	1.81	2[a]	0.0016	4.5	0.32
	U−O_{eq1}	2.27	2[a]	0.0075		
	U−O_{eq2}	2.48	3[a]	0.0056		
	U−S_{mon}	3.58	2[a]	0.0072		
	U−U	3.73	2[a]	0.011		

[a] Value fixed during the fit procedure. Errors in distances R are ±0.02 Å, errors in coordination numbers N are ±15%.

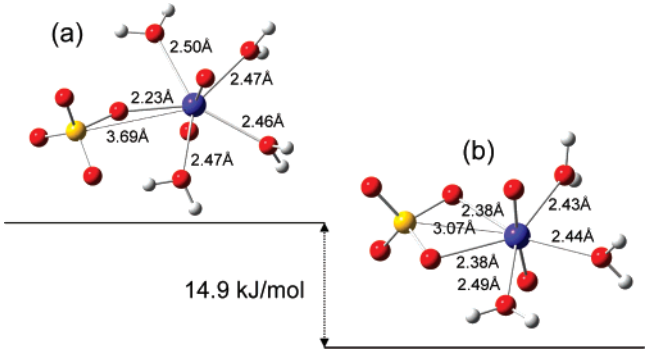

Figure 5. Structures of $UO_2SO_4(H_2O)_n$(aq) complexes optimized at the DFT level in solvent.

XRD, the EXAFS data show two sulfur atoms at a distance of 3.58 Å. The U−S_{mon} peak of the zippeite sample is clearly separated from the U−U peak at 3.73 Å. Therefore we conclude that EXAFS is able to reproduce the U−S_{mon} distance correctly, which is important for the discrimination of monodentate and bidentate sulfate.

DFT calculations were performed to optimize structures of U(VI) in 5-fold coordination including one sulfate group (Figure 5a and b). The calculations of monodentate $UO_2SO_4(H_2O)_4$(aq) complex (a) gives a U−S_{mon} distance of 3.69 Å and U−O_{eq} of 2.38 Å. The energy of the monodentate complex is 14.9 kJ mol^{-1} higher than the energy of the bidentate complex. Hence, DFT results suggest a bidentate coordination for the UO_2SO_4(aq) species, which is in contrast to the EXAFS results, suggesting a predominantly monodentate coordination. A difficulty in the comparison of DFT and EXAFS data is that DFT is related to an individual species, whereas EXAFS detects the average of the species distribution comprising UO_2^{2+}, UO_2SO_4(aq), $UO_2(SO_4)_2^{2-}$, and $UO_2(SO_4)_3^{4-}$. However, the energy difference between both types of coordination is close to the typical error limit of DFT calculations (±15 kJ mol^{-1}), and the small energy difference between monodentate and bidentate coordination may indicate the existence of different isomers in solution. From the structures of solids, it is well known that monodentate sulfate species tend to bridge two uranium atoms.[39−41] Furthermore, aqueous ternary U(VI) complexes occur already at pH ∼3. However, no indication for an U−U interaction at distances around 4 Å was found, suggesting the predominance of monomeric species only.

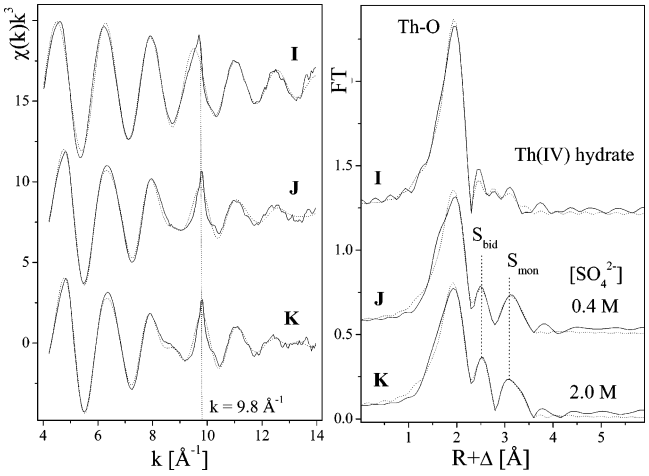

Figure 6. Th L_3-edge k^3-weighted EXAFS data (left) and the corresponding Fourier transforms (right) of Th(IV) hydrate and sulfato species. The dotted line in the EXAFS spectrum indicates the [2p4f] double-electron excitation.

In the previous section, we concluded that the structure of the dominant $UO_2(SO_4)_2^{2-}$ species prevailing at sulfate excess is associated with a bidentate sulfate coordination. In case of an equimolar ratio of $[SO_4^{2-}]$ and $[UO_2^{2+}]$, the thermodynamic speciation suggests that the dominant species is UO_2SO_4(aq) where a significant part of the sulfate is in monodentate coordination. These results allow interpretation of previously published contradictory results on U(VI) sulfate coordination as effect of the $[SO_4^{2-}]/[UO_2^{2+}]$ ratio. The bidentate U(VI) sulfate coordination found with EXAFS by Moll et al. was obtained for samples with a high $[SO_4^{2-}]/[UO_2^{2+}] > 10$.[7] Experiments with Raman spectroscopy of Nguyen-Trung et al., obtained from solutions with high $[SO_4^{2-}]/[UO_2^{2+}]$ ratio, i.e., 5−600, indicated also sulfate in a bidentate coordination mode.[8] In contrast, monodentate sulfate coordination was observed by Gal et al. with infrared spectroscopy[9] using $[SO_4^{2-}]/[UO_2^{2+}] < 3$. Neuefeind et al. observed with high-energy X-ray scattering monodentate coordination with $[SO_4^{2-}]/[UO_2^{2+}] = 1$.[10] We can summarize that the relation of isomers with monodentate and bidentate sulfate coordination is strongly affected by the $[SO_4^{2-}]/[UO_2^{2+}]$ ratio. At low $[SO_4^{2-}]/[UO_2^{2+}]$ ratio, the monodentate coordination prevails, whereas the bidentate coordination becomes dominant at a high $[SO_4^{2-}]/[UO_2^{2+}]$ ratio.

Th(IV) Complexes. In this section we discuss the structure of Th(IV) sulfato complexes. As reference a spectrum of Th(IV) hydrate is investigated. The k^3-weighted EXAFS function, $\chi(k)$, and the corresponding FT of samples **I**−**K** are shown in Figure 6; the corresponding fit results are summarized in Table 4.

Th(IV) Hydrate. The Th(IV) hydrate (sample **I**) is dominated by one intense peak resulting from the hydrate

(40) Burns, P. C.; Deely, K. M.; Hayden, L. A. *Can. Min.* **2003**, *41*, 687−706.

(41) Doran, M. B.; Norquist, A. J.; O'Hare, D. *Acta Crystallogr. E* **2005**, *61*, m881−m884.

Table 4. EXAFS Fit Parameters of Th(IV) Hydrate and Sulfato Complexes

sample	scattering path	R [Å]	N	σ^2 [Å^2]	$\Delta E_{k=0}$	F
I	Th−O	2.44	9.8	0.0068	−5.1	0.07
	Th−O_{II}	3.69	3.0	0.013		
J	Th−O	2.43	9.4	0.0093	−9.6	0.10
	Th−S_{bid}	3.14	0.9	0.0048[a]		
	Th−S_{mon}	3.80	3.7	0.0090[a]		
K	Th−O	2.42	9.2	0.0099	−9.7	0.11
	Th−S_{bid}	3.14	1.6	0.0048[a]		
	Th−S_{mon}	3.81	3.8	0.0090[a]		

[a] Value fixed during the fit procedure. Errors in distances R are ±0.02 Å, errors in coordination numbers N are ±15%.

oxygen atoms. The shell fit led to a phase-corrected distance of 2.44 Å, a coordination number of 9.8, and a Debye−Waller factor of 0.0068 Å.^{2} This result is in agreement with DFT calculations showing that each water molecule in the first hydration sphere binds, via its hydrogen atoms, two water molecules in the second hydration sphere and stabilizes a $[Th(H_2O)_n(H_2O)_{2n}]^{4+}$ cluster with $n = 9-10$.[42] Other publications, however, present controversial results: EXAFS analyses indicated hydration numbers of 9−11 (Moll et al.)[43] and 11.6−12.7 (Rothe et al.)[44] with a Th−O distance of 2.45 Å; a LAXS analysis suggested eight water molecules with a Th−O distance of 2.49 Å,[45] and NMR measurement indicated 9.1 water molecules in the first coordination sphere.[46]

The FT of sample **I** exhibits additional small peaks at higher R values. The spurious peak at $R + \Delta \approx 2.5$ Å is a FT side lobe arising from finite truncation of the experimental k range. In contrast, the peak at $R + \Delta \approx 3.3$ Å may have a physical origin. Giaquinta et al.[47] investigated Th(IV) sorbed onto bentonite with EXAFS and found a similar second oxygen shell at 3.66 Å. This shell was interpreted as a Th(IV)−clay interaction. Rothe et al.[44] observed such a Th−O peak at 3.66 Å in the Th(IV) hydrate species. Several scattering processes can be assumed to cause this peak: a single scattering Th−Cl path from a monodentately coordinated ClO_4^- group, a Th−Th scattering from Th polymers, or a single scattering Th−O path within the second hydration shell. Due to the low $[ClO_4^-]$ in sample **I**, an inner-sphere coordination is unlikely.[36] The Th−Th distances of 3.89 and 4.05 Å, reported for polymeric Th(IV) hydrolysis species,[48,49] are too long in comparison with the distance obtained here. The shell fit with a SS Th−O path gave $N_O = 3$, $R = 3.69$ Å, and $\sigma^2 = 0.013$ Å.^{2} However, this distance is too short in relation to the Th−O distance of water in the second hydration sphere which would be expected at a Th−O distance of 4.60 Å,[45] but it could be related with water molecules in interstitial positions.

Th(IV) Sulfate. The FT of Th(IV) sulfate solutions show three individual peaks which were fitted with one oxygen shell at 2.43 Å and two sulfur shells at 3.14 and 3.81 Å. For comparison, the coordination numbers and averaged Th−S distances of selected thorium sulfate crystal structures are summarized in Table S4 of the Supporting Information. The observed Th−S distances for bidentate sulfate are 3.12−3.19 Å and for monodentate sulfate 3.71−3.78 Å, suggesting that the solution comprises both bidentate and monodentate sulfate ligation. The solid compounds indicate also significant differences of the Th−O bond lengths for monodentate and bidentate sulfate groups. The Th−O distances of monodentate sulfate are 2.33−2.41 Å, and those of bidentate sulfate are 2.50−2.55 Å. Water molecules show Th−O distances of 2.48−2.59 Å in the crystal structures. The asymmetric broadening of the oxygen peak at $R + \Delta \approx 1.9$ Å is most likely due to these different distances in the first coordination shell, further supported by the large Debye−Waller factor of 0.0093−0.0099 Å.^{2} The distance resolution ΔR in the experimental k range, 0.16 Å, however, is not sufficient to fit the different distances of this shell.

The thermodynamic speciation indicates that the dominating species shifts from $Th(SO_4)_2(aq)$ to $Th(SO_4)_3^{2-}$ with increasing sulfate concentration. The EXAFS data showing an increase of coordinated sulfate are in qualitative agreement with this. When comparing the FT peak half-widths of the both sulfur peaks, it is obvious that those of S_{mon} are larger than that of S_{bid}. The reason might be that a bidentate coordination with its two bridging O bonds is more rigid against thermal movements than a single monodentate bond. Furthermore, the angle α of monodentate sulfate is in the order of ∼140° which is more susceptible to multiple scattering than the angle α ≈ 100° in bidentate sulfate (see Scheme 1). Both physical effects are reflected by the higher Debye−Waller factor for the monodentate coordination ($\sigma^2_{Smon} = 0.0090$ Å^2) in comparison to the bidentate coordination ($\sigma^2_{Sbid} = 0.0048$ Å^2). In the final curve-fits, the Debye−Waller factors have been fixed to keep the coordination numbers comparable among the sample series. As the $[SO_4^{2-}]$ increases, N_{Sbid} increases from 0.9 to 1.6, whereas N_{Smon} remains nearly unchanged.

U(IV) Complexes. U(IV) Hydrate. The EXAFS shell fit of U(IV) hydrate shows 8.7 oxygen atoms at a distance of 2.41 Å (Figure 7 and Table 5). A coordination number of 9 was also estimated with DFT.[24] Similar to Th(IV), a small peak at 3.47 Å is visible, which may be explained in analogy to Th(IV) hydrate.

U(IV) Sulfate. The FT of the aqueous solutions at pH 1 show two additional peaks at $R + \Delta \approx 2.5$ and 2.9 Å. These peaks could be fit with sulfur atoms at distances of ∼3.08 and 3.67 Å, indicating bidentate and monodentate sulfate coordination. Figure 8 shows the coordination number N_{Sbid} and N_{Smon} as a function of the sulfate concentration. The coordination number N_{Sbid} increases, whereas N_{Smon} decreases with increasing $[SO_4^{2-}]$. Hence, with increasing sulfate concentration the bidentate coordination becomes more

(42) Tsushima, S.; Yang, T. X.; Mochizuki, Y.; Okamoto, Y. *Chem. Phys. Lett.* **2003**, *375*, 204−212.
(43) Moll, H.; Denecke, M. A.; Jalilehvand, F.; Sandstrom, M.; Grenthe, I. *Inorg. Chem.* **1999**, *38*, 1795−1799.
(44) Rothe, J.; Denecke, M. A.; Neck, V.; Muller, R.; Kim, J. I. *Inorg. Chem.* **2002**, *41*, 249−258.
(45) Johansson, G.; Magini, M.; Ohtaki, H. *J. Solution Chem.* **1991**, *20*, 775−792.
(46) Fratiello, A.; Lee, R. E.; Schuster, R. E. *Inorg. Chem.* **1970**, *9*, 391−392.
(47) Giaquinta, D. M.; Soderholm, L.; Yuchs, S. E.; Wasserman, S. R. *J. Alloys Compounds* **1997**, *249*, 142−145.
(48) Skanthakumar, S.; and Soderholm, L. *Mat. Res. Soc. Symp. Proc.* **2006**, *893*, 411−416.
(49) Wilson, R. E.; Skanthakumar, S.; Sigmon, G.; Burns, P. C.; Soderholm, L. *Inorg. Chem.* **2007**, *46*, 2368.

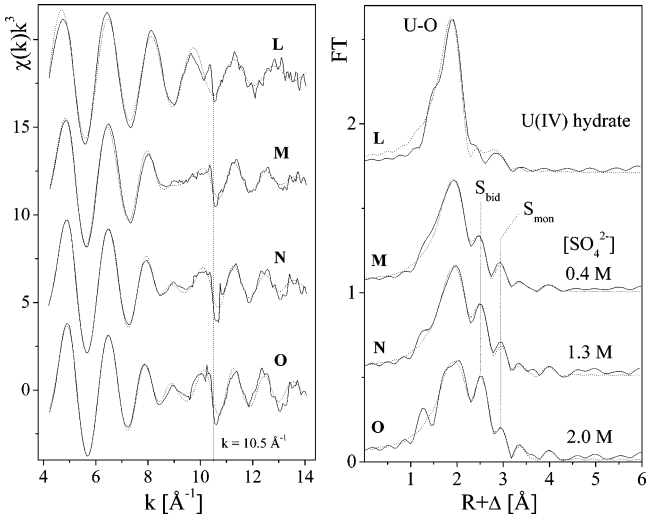

Figure 7. U L_3-edge k^3-weighted EXAFS data (left) and the corresponding Fourier transforms (right) of U(IV) hydrate and sulfato species. The dotted line in the EXAFS spectrum indicates the [2p4f] double-electron excitation.

Table 5. EXAFS Fit Parameters of U(IV) Hydrate and Sulfato Complexes

sample	scattering path	R [Å]	N	σ^2 [Å^2]	$\Delta E_{k=0}$	F
L	U−O	2.41	8.7	0.0070	−10.2	0.13
	U−O_{II}	3.47	3.2	0.0091		
	U−O	2.40	9.3	0.011	−9.8	0.10
M	U−S_{bid}	3.07	1.5	0.0048[a]		
	U−S_{mon}	3.67	2.5	0.011		
	U−O	2.40	9.1	0.012	−8.7	0.09
N	U−S_{bid}	3.08	2.0	0.0048[a]		
	U−S_{mon}	3.67	2.3	0.011		
	U−O	2.40	9.3	0.013	−8.3	0.10
O	U−S_{bid}	3.08	2.4	0.0048[a]		
	U−S_{mon}	3.67	2.2	0.011		
P	U−O	2.44	6.1	0.015	−7.6	0.11
	U−S_{mon}	3.66	2.8	0.0086		
	U−U	3.87	2.1	0.0073		

[a] Value fixed during the fit procedure. Errors in distances R are ±0.02 Å, errors in coordination numbers N are ±15%.

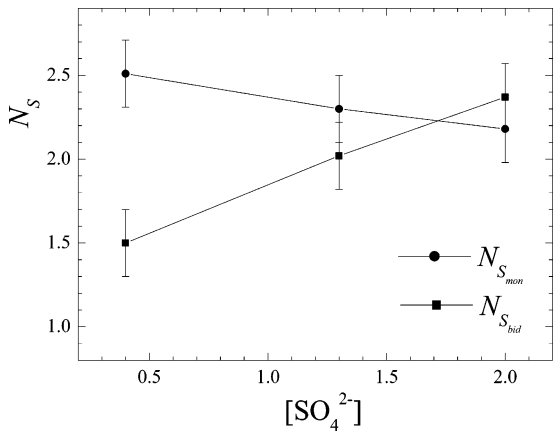

Figure 8. U(IV) sulfate coordination at pH 1. Number of sulfur neighbors N_{Sbid} and N_{Smon} as function of [SO_4^{2-}].

dominant. It should be noted that under comparable experimental conditions the spectrum of Th(IV) sulfate yields larger FT peaks from monodentate sulfate in comparison to that of the U(IV) sulfato species. The Debye−Waller factor of the coordinating sulfato U−O shell is significantly higher than that of the pure U(IV) hydrate and increases slightly with increasing sulfate concentration. According to the general tendency observed in the crystal structures, the U−O distance of monodentate sulfate is expected to be shorter than that of the bidentate sulfate. Therefore, a shell fit was performed with two U−O subshells. The fit with fixed σ^2 values of 0.007 Å^2 yielded two U−O distances of 2.28 and 2.41 Å. However, the difference ΔR of these two subshells, 0.13 Å, is smaller than the distance resolution ΔR of 0.16 Å in the available k range. Therefore, the two subshells are not considered in Table 5.

The difference in the interatomic distances of U(IV) and Th(IV) sulfato complexes reflects the difference of their ionic radii, $R_{Th(IV)} = 1.23$ Å, and $R_{U(IV)} = 1.19$ Å.[50] The known solid U(IV) sulfates show exclusively 8-fold coordination and only monodentate sulfate groups, whereas the known solid Th(IV) sulfates comprise coordination numbers of 8, 9, and 10, as well as monodentate and bidentate sulfate groups (Supporting Information, Table S4). However, the similarity of the ionic radii makes isomorphous crystal structures like $U(SO_4)(OH)_2$ and $Th(SO_4)(OH)_2$ possible.[51,52] From the structure parameters in solution, it can be expected that also solid U(IV) structures with bidentate sulfate may exist.

In contrast to the stoichiometry proposed by the EXAFS results, the thermodynamic modeling of the U(IV)−sulfate interactions predicts the predominance of the neutral $U(SO_4)_2$-(aq) complex. Independent of the sulfate concentration and without considering the coordination mode, the EXAFS measurements indicate sulfate coordination numbers of 4.0 and 4.8 for samples **M** and **O**, respectively.

The electrochemical conversion of U(VI) to U(IV) transforms the trans-dioxo cation UO_2^{2+} to the spherically coordinated U^{4+} cation. The EXAFS measurements show that the loss of the trans-dioxo cations is accompanied by a rearrangement of coordinating sulfate ions. In presence of the trans-dioxo cations of U(VI), the sulfate coordination is restricted to the equatorial plane, whereas the U(IV) cations provide the whole sphere for the coordination. In 2 M [SO_4^{2-}] solution, U(VI) is dominated by bidentate coordination, whereas U(IV) comprises both bidentate and monodentate sulfate ions. This difference may reflect sterical restrictions in the coordination sphere of U(VI) with its trans-dioxo cations. Interesting is the comparison with Pa(V) in 13 M H_2SO_4 solution that contains only one oxo cation.[53] Pa(V) is coordinated by two bidentate sulfate groups with a U−S distance of 3.09 Å and three monodentate sulfate groups at 3.73 Å. In contrast, Np(IV) in 0.1 M HNO_3 and 2 M H_2SO_4 is coordinated exclusively by two bidentate sulfate ions at a Np−S distance of 3.07 Å.[54] These examples indicate that the sulfate coordination of actinides is affected not only

(50) Shannon, R. D. *Acta Crystallogr. A* **1976**, *32*, 751−767.
(51) Lundgren, G. *Arkiv foer Kemi* **1952**, *4*, 421−428.
(52) Lundgren, G. *Arkiv foer Kemi* **1950**, *2*, 535−549.
(53) Le Naour, C.; Trubert, D.; Di Giandomenico, V.; Fillaux, V.; Den Auwer, C.; Moisy, P.; Hennig, C. *Inorg. Chem.* **2005**, *44*, 9542−9546.
(54) Reich, T.; Bernhard, G.; Geipel, G.; Funke, H.; Hennig, C.; Rossberg, A.; Matz, W.; Schell, N.; Nitsche, H. *Radiochim. Acta* **2000**, *88*, 633−637.

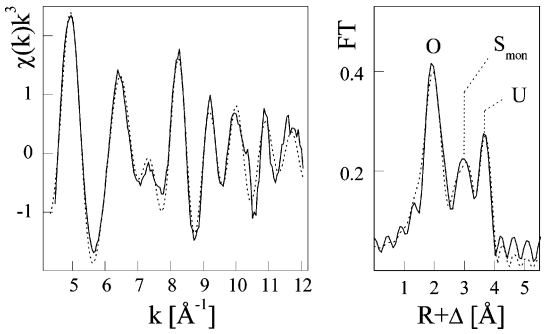

Figure 9. U L_3-edge k^3-weighted EXAFS data and their Fourier transform of U(IV) precipitate (**P**).

by the metal to sulfate ratio, the pH value, and the ionic strength but also by the number of oxo cations that may restrict the coordination.

U(IV) Sulfate Precipitate. An amorphous U(IV) precipitate (sample **P**) was investigated with EXAFS in order to get information on the solid-state sulfate coordination (Figure 9 and Table 5). The chemical composition (458.0 mg/g U, 59.7 mg/g Na, 64.0 mg/g SO_4^{2-}) indicates a basic sulfate.[55] There are three dominant FT peaks that were identified as U−O at 2.44 Å, U−S at 3.66 Å, and U−U at 3.87 Å. No peak arises at $R + \Delta \approx 2.5$ Å that could be related to bidentate sulfate coordination. The EXAFS data indicate a rearrangement of the coordinated sulfate groups from a mixed monodentate/bidentate coordination in solution to a monodentate coordination in solid state. The appearance of the U−U peak at 3.87 Å in the precipitate indicates a polmerization via −O− or −OH− bridges. The absence of any similar U−U interaction for the solution species indicates that the U(IV) sulfato complex appears there as monomer.

Conclusion

The apparent discrepancies in the literature with respect to an either monodentate or bidentate coordination of UO_2^{2+} aquo sulfato complexes could be resolved as an effect of the $[SO_4^{2-}]/[UO_2^{2+}]$ ratio. At low $[SO_4^{2-}]/[UO_2^{2+}]$ ratio (∼1), monodentate sulfate coordination and the UO_2SO_4(aq) species prevails. At high $[SO_4^{2-}]/[UO_2^{2+}]$ ratio, however, bidentate sulfate coordination and the $UO_2(SO_4)_2^{2-}$ species prevail in line with the thermodynamic estimations; $UO_2(SO_4)_3^{4-}$ is under the chosen experimental conditions always of minor importance.

U(VI), U(IV), and Th(IV) sulfate samples comprise sulfate in both monodentate and bidentate coordination. An exclusively bidentate coordination was observed only for U(VI) at a high $[SO_4^{2-}]/[UO_2^{2+}]$ ratio. The correlation between the thermodynamic species and the sulfate coordination is less clear for U(IV) and Th(IV), which is at least in part due to the lack of higher formation constants. In general, in all systems the bidentate coordination becomes dominant with increasing sulfate coordination.

The coordination structure was derived by EXAFS measurements from the position and intensity of the U−S peaks. In contrast to the U−O backscattering signals, which suffer from unresolved superposition, the U−S peaks are well separated and therefore appropriate for a quantitative analysis.

Acknowledgment. We greatly acknowledge Prof. R. Vochten, University of Antwerp, Belgium, who provided the zippeite sample. The EXAFS measurements were performed at the Rossendorf Beamline/ESRF. This work was supported by the DFG under contract HE 2297/2-1. S.T. was supported by the stipend from the Alexander-von-Humboldt foundation. Generous allocation of computation time on supercomputers at Zentrum für Informationsdienste and Hochleistungsrechnen (ZIH), Technische Universität Dresden, Germany, is gratefully acknowledged.

Supporting Information Available: Listings of EXAFS spectra and fit results of U(VI) sulfate at pH 2 used for Figure 2; coordinates of all DFT calculations for the complex structures. This material is available free of charge via the Internet at http://pubs.acs.org.

IC0619759

(55) Perez, F. M.; Gil, J. M.; Gil, F. J. M. *Z. Anorg. Allg. Chem.* **1980**, *462*, 231−240.